

IN-SITU X-RAY MICRODIFFRACTION STUDY OF SINGLE SLIP CONDITIONED COPPER POLYCRYSTALS DURING UNIAXIAL DEFORMATIONS

H.D. Joo*, J.S. Kim, C.W. Bark*, J.Y. Kim*, Y.M. Koo*, and N. Tamura†

* *Materials Sci. & Eng., Pohang University of Science and Technology, Pohang 790-784, South Korea,*

† *Lawrence Berkeley National Laboratory, University of California, 1 Cyclotron Road, Berkeley, CA 94720, USA*

ABSTRACT

Recent experiments have shown that formation of dislocation cell structures and rotation of structural elements at the macroscopic level are fundamental to the development of plastic deformation. However, attention should also be focused on micro-volumes because local stress and strain can significantly differ from their averaged values at the macroscale. *In-situ* orientation measurements in copper polycrystals during uniaxial deformation were performed using synchrotron x-ray microdiffraction at the Advanced Light Source. The intergranular heterogeneities of the deformation-induced microstructure were obtained. The shape of the intensity profile and the direction along elongated streaks in the Laue image are obtained at different positions of grain interior. The differences in the selection of simultaneously acting slip systems and that of dislocation arrangements among the intergranular and the intragranular level are discussed.

§1. INTRODUCTION

The deformation of polycrystalline materials is very heterogeneous both at the intergranular and the intragranular level. Recent experiments have shown that formation of dislocation cell structure and rotation of structural elements at the macro-level are fundamental to the development of plastic deformation and fracture of solids[1,2]. During plastic deformation, regions within a grain are delineated by dense dislocation walls as undissociated dislocation boundaries separating volumes with simultaneously operating slip system.[1] Each region has different operating slip system. Deformation pattern within each region is quite homogeneous, but different from the patterns in neighboring region. Further subdivision of grain takes place at the higher strain. However, *in-situ* study of deformation behavior in polycrystals at mesolevel has not been performed. In the present work, the intergranular heterogeneities of the deformation-induced microstructure were obtained. The shape of the intensity profile and the direction along elongated streaks in the Laue image are obtained

at different positions of grain interior. The differences in the selection of simultaneously acting slip systems and that of dislocation arrangements among the intergranular and the intragranular level are discussed

Notation: Slip planes and directions are referenced according to the Schmid and Boas notation.[5]

Plane \Rightarrow B={111}, A= $\bar{1}$ 11}, C= $\bar{1}$ $\bar{1}$ 1}, D={1 $\bar{1}$ 1};

Direction \Rightarrow I=[011], II=[0 $\bar{1}$ 1], III=[101], IV= $\bar{1}$ 01}, V= $\bar{1}$ $\bar{1}$ 0}, VI=[110]

§2. EXPERIMENTAL PROCEDURE

The material used in the present study was a 99.999% polycrystalline copper. A tensile sample, with a 7.5 mm gauge length and a 2 mm x 0.5 mm cross-section, was prepared by spark-erosion cutting. After mechanical polishing, the sample was annealed at 500°C and chemically polished. We used synchrotron X-ray microdiffraction end-station on beamline 7.3.3 at the Advanced Light Source (ALS) to perform *in-situ* micro-diffraction experiments [3]. Due to the 45° incidence of the X-ray, the actual beam size at the sample position was 1.5 μm * 1.5 μm . In order to map the orientation and strain/stress distributions for each strain (0, 2, 4, 6, 8, 10, 15, 20, 25% strain), the same area on the sample was repeatedly raster scanned with the x-ray microbeam with a step size of 4 microns. The samples were elongated by a tensile device mounted on the translation stage with a strain rate of $2.22 \times 10^{-4} \text{ s}^{-1}$.

§3. RESULTS AND DISCUSSIONS

Diffraction patterns obtained from sample different positions were indexed and the orientation

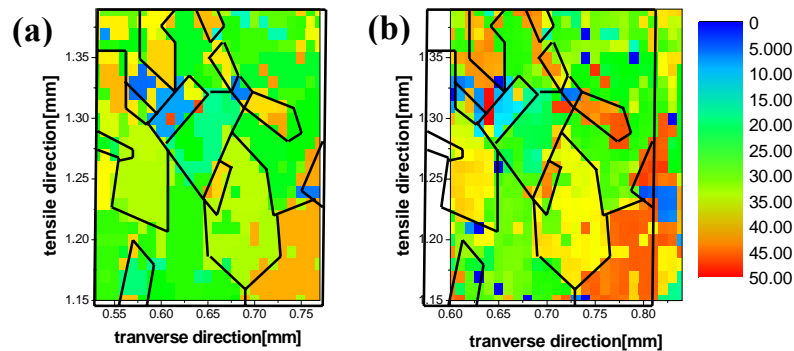


Figure 1. (a) and (b) show the orientation maps of the central grain at 0 and 8% strain, respectively, where the y direction is the sample tensile direction..

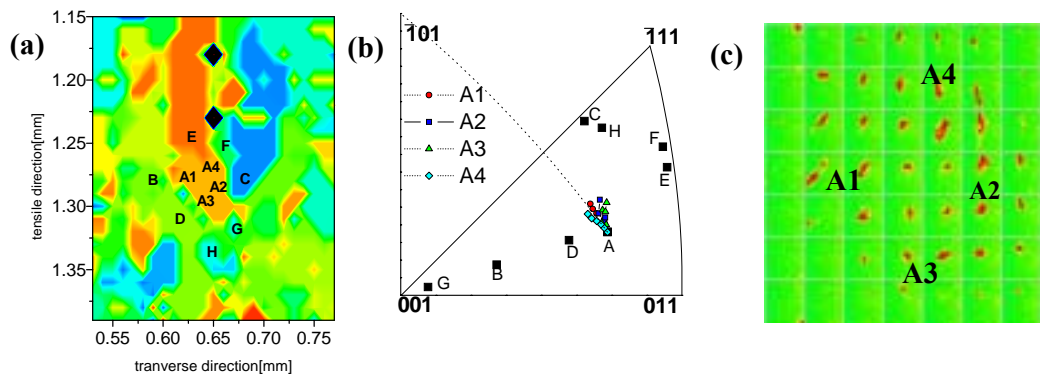


Fig. 2. (a) The orientation map of the sample, and (b) tensile axis movements of 4 other points in the center grain in standard stereographic triangle are shown. (c) The mosaic image of the 024 peak of each diffraction pattern at 6% strain is shown.

matrices were deduced. The orientation map was obtained by the following steps; the first step is to obtain diffraction pattern at each point by raster scan of which step size is $10\mu\text{m}$, the second step is to index all diffraction patterns, and the last step is to calculate the angle between a certain peak like (111) and tensile axis and make orientation map. The orientation distributions in the copper samples at 0 and 8% strain are shown in Fig. 1. The misorientation measured within the central grain before loading is less than 0.1 degree, and increases in function of the applied tensile strain. We observed a higher variation in orientation by increasing strain in the middle of the center grain than at other positions within this grain.

The orientations of several grains in Cu sample and tensile axis movement of 4 other points in the center grain in standard stereographic triangle are measured and shows in Fig. 1(a) and (b), where the points show the experimental data, while the dotted line represents the expected path for the tensile axis as predicted by Schmid's law[4]. Tensile axis movements like that of position A1, follow expected classical theory tensile axis paths, but rotation angles varied differently. According to Schmid's law, initially activated slip systems in single crystals would have the highest Schmid factor [4]. The tensile axis follows the expected path for the BIV(111)[$\bar{1}01$] slip system (described by the Schmid and Boas notation.[4]), as in a single crystal but the total rotation angle from the initial orientation depends on the location within the grain. This may mean that multi-slip systems are activated and different slip systems are operated in each position.

The streaking of diffraction patterns is considered in order to investigate the type of geometrically necessary unpaired dislocation. The mosaic image of the 024 peak from each diffraction pattern in center grain region is obtained and shows in Fig. 1(c). The shape of 024 peaks depends on position within center grain. The directions of peak broadening are diagonal direction at

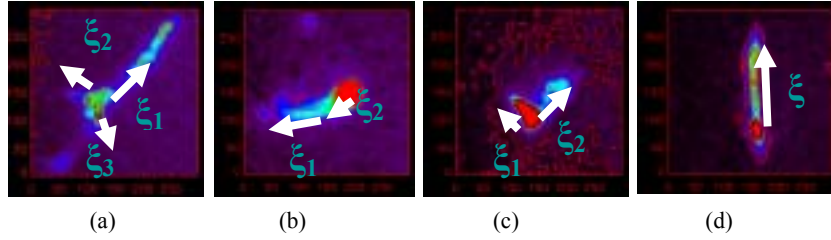


Figure 3. Laue images of the (024) reflection in the CCD plane for 8% strained Cu crystals. (a), (b), (c), and (d) are the reflections of the A1, A2, A3, and A4 position of the central grain, respectively. The calculated Burgers vector(b) and dislocation line vector(τ) are (a) $b_1//[-110]$, $\tau_1//[11-2]$, $b_2//[110]$, $\tau_2//[-1-12]$, $b_3//[-110]$, $\tau_3//[112]$, (b) $b_1//[-101]$, $\tau_1//[1-21]$, $b_2//[-110]$, $\tau_2//[112]$, (c) $b_1//[-101]$, $\tau_1//[1-21]$, $b_2//[011]$, $\tau_2//[21-1]$, (d) $b//[0-11]$, $\tau//[2-1-1]$.

A1 region and vertical direction in A4 region. The separated peak is observed in high strain condition, which may be caused by forming dislocation cell structure. The dislocation structure was analyzed based on the approach described by Barabash et al.[6]. That model restricts three following unpaired dislocation: 1) geometrically necessary boundary (GNB) formed by tilt dislocation boundary, 2) incidental dislocation boundaries (IDB), and 3) individual geometrically necessary dislocation (GND). According to that model, the unpaired dislocation makes the streaking of diffraction peak, and dislocation arrangements can be identified by analyzing streaked peak. In fcc crystals, there are 12 slip systems which have typical edge dislocation lines parallel to the direction of $\langle 112 \rangle$ with Burgers vector parallel to the glide direction $\langle 110 \rangle$ and with corresponding glide planes $\{111\}$. Several Laue peaks with streaking axes parallel to $\xi = \tau \times g / |\tau \times g|$, where τ is the dislocation line vector and g is the momentum transfer vector. The streaking directions are simulated about the 12 most likely edge dislocation systems and compared with the experimental one. In this way, we determined the kind of dislocation system, as shown in Fig.3. Unpaired dislocations piled-up in the A1 position of the central grain has a Burgers vector $b = [-110]$, dislocation line $\tau = [11-2]$ and slip plane $n = (111)$ which corresponds to the BV slip system. Dislocation types of Reflection tail correspond to AVI and CVI, that is, multi-slip systems have been activated. Especially separation of peak is observed at ξ_1 direction. That means BV dislocation system is location in tilt dislocation boundary and the other dislocation is randomly distributed individual unpaired dislocation. This phenomenon can be observed in A4 position. BII dislocation is not only located in tilt dislocation boundary but randomly distributed. Tensile axis rotations of 4 other positions also follow the BIV slip system, but there is little deviation which results from multi-slip. The dislocations system of A2, A3, and A4 position in the central grain correspond to BVI, CV, D1 and B2 slip systems. In this case, other slip system are

activated, glide path may be another important factor to determine the operative slip system.

In summary, we have investigated the effect of neighboring grains on intra-/inter-granular plastic deformations during uniaxial deformation by *in-situ* observation of local lattice rotation and diffraction peak streaking.

ACKNOWLEDGEMENTS

This work was done as a part of the Nanotechnology Development Program supported by Ministry of Science & Technology, republic of Korea. We thank R.S. Celestre and W.A. Caldwell for their assistance in performing the Microdiffraction experiment at the Advanced Light Source. The Advanced Light Source is supported by the Office of Science, Office of Basic Energy Sciences, Materials Sciences Division, of the U.S. Department of Energy under Contract No. DE-AC03-76SF00098 at Lawrence Berkeley National Laboratory.

REFERENCE

1. N. Hansen,; *Mater. Sci. Engng*, Vol.6 (1990), p. 1039
- 2 S. A. Gernov, D. Hamana, N.A. Dvorovienko, V.L. Golayev, and V.M. Tchmutov: *Phil. Mag. Lett* : Vol. 78 (1998), p. 185
3. A. A. MacDowell, R. S. Celestre, N. Tamura, R. Spolenak, B. Valek, W.L. Brown, J.C. Bravman, H.A. Padmore, B. W. Batterman, and J.R. Patel: *Nuclear inst. Meth.*, Vol 467-468 (2001), p. 936
4. E. Schmid, and W. Boas, *Plasticity of Crystals* (London: Chapman & Hall); translation of original 1935 German edition, 1968
5. E. Schmid and N. Boas, *Kirstall. Plastizitat*, Berlin (1961)
6. R.I. Barabash, G.E. Ice, and F.J. Walker, *J. Appl. Phys.*, 93 (2003), p. 1457